Clim. Past Discuss., 3, 1283–1309, 2007
www.clim-past-discuss.net/3/1283/2007/

Climate of the Past Discussions

Climate of the Past Discussions is the access reviewed discussion forum of *Climate of the Past*

Climate fluctuations during the Holocene in NW Iberia: high and low latitude linkages

L. D. Pena[1], G. Francés[2], P. Diz[2], M. A. Nombela[2], and I. Alejo[2]

[1]GRC Geociències Marines, Department de Estratigrafía, Paleontología i Geociències Marines, Universitat de Barcelona, C/ Martí i Franqués, s/n, 08028 Barcelona, Spain
[2]Departamento de Xeociencias Mariñas e Ordenación do Territorio, Facultade de Ciencias do Mar, Universidade de Vigo, As Lagoas-Marcosende, s/n, 36310 Vigo, Spain

Received: 13 November 2007 – Accepted: 22 November 2007 – Published: 3 December 2007

Correspondence to: L. D. Pena (lpena@ub.edu)

Abstract

High resolution benthic foraminiferal oxygen and carbon stable isotopes ($\delta^{18}O$, $\delta^{13}C$) from core EUGC-3B are used here to infer rapid climatic changes for the last 8500 yr in the Ría de Muros (NW Iberian Margin). Benthic foraminiferal $\delta^{18}O$ and $\delta^{13}C$ potentially register migrations in the position of the hydrographic front formed between two different intermediate water masses: Eastern North Atlantic Central Water of subpolar origin ($ENACW_{sp}$), and subtropical origin ($ENACW_{st}$). The isotopic records have been compared with two well established North Atlantic marine Holocene paleoceanographic records from low (Sea Surface Temperatures anomalies off Cape Blanc, NW Africa) and high latitudes (Hematite Stained Grains percentage, subpolar North Atlantic). This comparison clearly demonstrates that there is a strong link between high- and low-latitude climatic perturbations at centennial-millennial time scales during the Holocene. Spectral analyses also points at a pole-to-equator propagation of the so-called 1500 yr cycles. Our results demonstrate that during the Holocene, the NW Iberian Margin has undergone a series of cold episodes which are likely triggered at high latitudes in the North Atlantic and are rapidly propagated towards lower latitudes. Conceivably, the propagation of these rapid climatic changes involves a shift of atmospheric and oceanic circulatory systems and so a migration of the hydrographical fronts and water masses all along the North Atlantic area.

1 Introduction

In recent years, many researchers have documented the existence of a series of recurring millennial-scale cooling events in North Atlantic deep sea sediments (Bond et al., 1997, 2001; Bianchi and McCave, 1999; Keigwin and Boyle, 2000; Giraudeau et al., 2001; Andrews et al., 2003; Marchitto and deMenocal, 2003; Oppo et al., 2003; Solignac et al., 2004) and Subtropical Atlantic (deMenocal et al., 2000a, b; Keigwin and Boyle, 2000) with a mean periodicity around 1500±500 years. This sub-

Milankovitch climate variability has also been recognized in pollen records, lacustrine deposits (Campbell et al., 1998; Viau et al., 2002; Hu et al., 2003) and speleothems (McDermott et al., 2001). A distinctive feature that characterizes this pervasive cycle is that it operates irrespective of whether the system is in a glacial or an interglacial mode (Bond et al., 1997, 1999; deMenocal et al., 2000b). Although increasing documentation of these quasi-periodic cycles during the Holocene has arisen from records around the world, there is a considerable debate regarding their timing (Schulz and Paul, 2002), driving force (Bond et al., 2001) and the mechanism that propagates these Holocene climatic perturbations in the atmosphere-ocean system. It has been argued that subtle changes in the Atlantic Meridional Overturning Circulation (MOC) may have played a major role in the amplification of these millennial scale events due to changes in meridional heat transport (Marchitto and deMenocal, 2003; Oppo et al., 2003) and that a partial shut-down of the thermohaline circulation (THC) might have triggered and/or amplified Late Holocene cold episodes, as for example the Little Ice Age (LIA) in the North Atlantic (Keigwin and Boyle, 2000).

Marine shallow areas and continental shelves have a great potential as high resolution paleo-archives, yet little attention has thus far been directed to these areas owing to the difficulty to discriminate between local and global climatic-oceanographic changes in the past. In this sense, the NW Iberian Margin has proved to be particularly sensitive to short time-scale changes during the late Holocene, both hydrographical (Diz et al., 2002; Álvarez et al., 2005; González-Álvarez et al., 2005) and atmospheric changes (Martínez-Cortizas et al., 1999; Desprat et al., 2003). However, whether these climatic changes are local or a response to a global forcing is still a matter of debate (Diz et al., 2002; Álvarez et al., 2005; González-Álvarez et al., 2005). Therefore, more effort needs to be directed toward these especially sensitive regions, in order to obtain high resolution Holocene records with potential to resolve climatic and oceanographic changes at centennial and millennial time scales.

In this study we analysed the stable oxygen and carbon ($\delta^{18}O$, $\delta^{13}C$) isotopic composition of benthic foraminifera from a core located in the Ría de Muros (NW Iberian

Peninsula), a shallow marine environment with relatively high sedimentation rates. The gravity core EUGC-3B records the last 8200 cal. yr BP. The Ría de Muros is located in the vicinity of the Finisterre Front, a hydrographic front between two components of the Eastern North Atlantic Central Water (subpolar and subtropical end-members, ENACWsp and ENACWst, respectively) and thus it is a potential area for recording past oceanographic fluctuations at centennial and millennial time-scales. In order to determine the possible linkages with general and widespread climatic patterns in the North Atlantic during the Holocene, we compare our record with previously published North Atlantic Holocene records which are known to reflect centennial-millennial scale variability: SST anomaly off Cape Blanc, Hole 658C (Bond et al., 1997, 1999; deMenocal et al., 2000b) and Hematite Stained Grains percentage (HSG), VM 29-191 (Bond et al., 1997, 1999; deMenocal et al., 2000b).

2 Study area and regional oceanography

The Ría de Muros is the northernmost of the so-called Rías Baixas, a set of funnel-shaped shallow incised valleys that distinguish the NW Iberian coasts (Fig. 1a-c). They are under the direct influence of shelf winds that modify the typical two-layer residual circulation pattern characteristic of partially mixed estuaries (Álvarez-Salgado et al., 2000). During the upwelling favourable season (April–September) cool and nutrient-rich intermediate waters (ENACW) are advected into the Rías Baixas significantly increasing the primary production in the surface waters and the flux of organic carbon to the sediment and also to the adjacent continental shelf (Prego, 1993; Rosón et al., 1999; Álvarez Salgado et al., 2001). Consequently, during relatively strong or persistent upwelling periods, a large fraction of the organic materials produced within the Rías is exported to the continental shelf, thus contributing to the rapid aging of the upwelled ENACW (Álvarez-Salgado et al., 2000). Conversely, during the rest of the year, downwelling-favourable southerly winds prevail and the circulation pattern reverses accumulating surface waters into the outer areas of Rías Baixas and preventing the entrance of ENACW. Downwelling periods are characterized by lower water renewal rates, consumption of nutrients and in situ organic matter degradation (Álvarez-Salgado et al., 2000).

The Galician continental shelf is hydrographically characterized by the presence of two different intermediate water masses that converge off Cape Finisterre (Fraga, 1991; Pérez et al., 1993, Figs. 1d–e): ENACW of subtropical origin ($ENACW_{st}$) and ENACW of subpolar origin ($ENACW_{sp}$). $ENACW_{st}$ can be easily identified in a Temperature/Salinity plot as a straight line ranging from 13.13°C, 35.80 psu (practical salinity units) to 18.50°C and 36.75 psu (Fiúza, 1984) (Figs. 1d–e). $ENACW_{st}$ is formed near 35° N along the Azores Front as a result of the subduction of large water volumes due to local evaporation processes and the subsequent winter surface cooling (Fiuza, 1984). After water mass formation, $ENACW_{st}$ is advected eastward by the Azores Current to be finally split into two different branches: one spreads southward to north-western Africa and the other one northwards reaching the occidental margin of the Iberian Peninsula more aged and progressively less oxygenated (Pérez et al., 2001, Fig. 1f). As a consequence, $ENACW_{st}$ is relatively less oxygenated than $ENACW_{sp}$ at the area of convergence between both water masses at Finisterre Front (see Fig. 1f). The $ENACW_{sp}$ is relatively colder and less saline than the $ENACW_{st}$ and can be identified in a T-S plot as a straight line between 10.0°C, 35.40 psu and 12.20°C, 35.66 psu (Figs. 1d–e). This water mass is formed in the Northeast Atlantic along the 46° N parallel (Celtic Sea) due to winter cooling and deep convection (McCartney and Talley, 1982). These hydrographical models (Fiúza, 1984) have been subsequently confirmed by many others authors (Ríos et al., 1992; Álvarez-Salgado et al., 1993, 1997, 2003; Castro et al., 1994; Pérez et al., 2001; Peliz et al., 2002). The convergence of this water masses develops in a subsurficial hydrographic front with the $ENACW_{st}$ to the south and the $ENACW_{sp}$ to the north (Fraga, 1991; Pérez et al., 1993) (Figs. 1d–e). The convergence of water masses together with northerly prevailing winds cause a quasi-permanent summer upwelling of nutrient rich waters. The regional position of this front varies in short time scales (annual/interannual) migrating northward and southward depending on regional climatology and oceanographic factors (Álvarez-Salgado et al., 1993) and thus deciding the upwelling of either $ENACW_{st}$ or $ENACW_{sp}$ (Álvarez-Salgado et al., 1993, 1997; Pérez et al., 2001). This mechanism could have operated likewise on longer time scales (centennial-millennial), with both $ENACW_{st}$ and/or $ENACW_{sp}$ upwelling accordingly to general northward or southward shifts of hydrographical fronts in the North Atlantic.

3 Material and methods

3.1 Stable isotopes analyses

Gravity core EUGC-3B (42° 45.105′N, 9° 02.231′W; 412 cm long, 38 m depth) was recovered within the framework of the EU HOLSMEER project during the 2001 BIO Mytilus cruise. The upper part of the core (2.5–0 m) was sampled at 2 cm intervals and the lower part (4.1–2.5 m) at 3–4 cm intervals. As a general sampling routine, the outer rind of the core was removed, hence avoiding possible sources of contamination from the sedimentary column that often take place during core retrieval. Bulk sediment subsamples were oven dried, weighed and soaked in a disaggregating solution and then wet sieved over a >125 μm sieve. Between 15 and 25 specimens of the benthic foraminifera Nonion commune (d'Orbigny) were picked from the >125μm fraction for stable isotopic (δ^{18}O, δ^{13}C) measurements. Only well preserved individuals (without clear signals of test alteration and/or partial dissolution) were selected for these analysis. All samples were firstly sonicated in distilled water in order to remove potentially attached clays from the foraminiferal tests.

The relatively high abundance of N. commune along the core (Lebreiro et al., 2006) and its shallow infaunal preferential habitat (Diz and Francés, in press) make this species a excellent candidate for the paleoceanographic reconstruction of the selected area all through the Holocene. Stable carbon and oxygen isotope measurements were carried out at the University of Bremen (Geosciences Faculty) using a FINNIGAN MAT

251 mass spectrometer coupled online with a Kiel automated carbonate preparation device. Long term reproducibility was calculated using an internal standard (Solnhofen Limestone) routinely measured over several months (±0.07‰ for $\delta^{18}O$ and ±0.05‰ for $\delta^{13}C$). All the isotopic data were referred to the Vienna Pee Dee belemnite standard (V-PDB scale).

3.2 Age model of core EUGC-3B

The age model was established by means of accelerator mass spectrometry (AMS) radiocarbon dating of seven intervals (Table 1) at the AMS Laboratory, Institute of Physics and Astronomy (University of Aarhus, Denmark). One benthic foraminiferal sample and 6 well preserved bivalve shells (e.g. unbroken, both valves still articulated, delicate structures preserved) were selected for ^{14}C AMS dating. All species are characterized by very shallow infaunal habitat preferences (Table 1). Raw radiocarbon ^{14}C ages were calibrated to calendar ages with the Calib 5.01 software (Stuiver and Reimer, 1993) using the MARINE04 calibration curve (Hughen, 2004). Radiocarbon dates and calibrated ages (with ±2 sigma ranges) are listed in Table 1. All the ages in this paper are expressed in calendar years BP unless otherwise specified. The age model was calculated by linear interpolation between the calibrated ages of the dated levels (Figs. 2a) resulting on average sedimentation rates of 0.049 cm/yr with intervals of up to 0.137 cm/yr.

3.3 Spectral analysis

We have developed a Continuous Wavelet Spectrum (CWS) analysis on the three selected data-sets: NW Iberia benthic $\delta^{13}C$ (EUGC-3B), SST anomaly off Cape Blanc (Hole 658C) and Hematite Stained Grains percentage in subpolar North Atlantic (HSG, VM 29-191) (Fig. 1a). The CWS is a multi-resolution time-frequency technique that is useful for exploring data known to be non-stationary (Torrence and Compo, 1998). With this approach we can examine possible changes in the nature of most important periodicities all along the time period of selected records. For this purpose we have selected a complex Morlet wavelet which offers great frequency resolution but is slightly less efficient in ascertaining time localization. Results are shown as 2-D contours of spectral variance (variance normalized CWS) in both time and frequency domains.

4 Results

4.1 Stable isotopes

Benthic foraminiferal $\delta^{13}C$ values range between −0.70‰ and −4.45‰ (Fig. 2, Fig. 3c) with an average value of −3.13‰. A detailed inspection of this record allows the identification of two distinctive intervals: the lower part (from ca. 8200 cal. yr BP to 3800 cal. yr BP) and the upper part (ca. 3800–536 cal. yr BP) (Figs. 2 and 3c). The older period shows a generally decreasing $\delta^{13}C$ trend that occurs in three major steps consisting of an initial depletion of the $\delta^{13}C$ values of about −1.3‰ are followed by relatively brief plateaus (Figs. 2 and 3c). The first step (8200–7314 cal. yr BP) is characterized by an initial rapid fall in the $\delta^{13}C$ values (from −0.30‰ to −1.60‰) which is followed by relatively stable plateau with an average ratio of −1.51‰. The second isotopic pulse (7314–6360 cal. yr BP) also took place with an initial depletion in the $\delta^{13}C$ values (from −1.60‰ to −2.58‰) and the corresponding plateau phase. Finally, the last step (6360–3735 cal. yr BP) presents a similar initial decrease in the $\delta^{13}C$ values (from −2.58‰ to −3.86‰) finishing with another $\delta^{13}C$ isotopic plateau averaging −3.89‰ (Fig. 2 and 3c). The upper part generally shows low $\delta^{13}C$ values that are interrupted by several abrupt events of rapid enrichments in the $\delta^{13}C$ values (Fig. 2 and 3c). In the first and most significant of these abrupt events (3735–2978 cal. yr BP), $\delta^{13}C$ values increase by 2.5‰ immediately after the core $\delta^{13}C$ minimum (−4.45‰). Afterwards, low $\delta^{13}C$ values are registered again in the record, presenting a slightly increasing trend towards more positive values from this point to the core top. Positive excursions also occur at 1804 and 1040 cal. yr BP. The uppermost part of the $\delta^{13}C$ record shows a rapid increase

CPD
3, 1283–1309, 2007

EGU

trend to positive values (Fig. 2 and 3c).

The overall $\delta^{18}O$ variability is much lower than that for the $\delta^{13}C$ record with $\delta^{18}O$ values ranging between 1.60‰ and 2.15‰ (Figs. 2 and 3a). Three main intervals can be distinguished (Figs. 2 and 3a). At the core bottom (8170–7331 cal. yr BP), the $\delta^{18}O$ record shows a sharp increase in the $\delta^{18}O$ values from 1.60‰to 1.99‰. After this brief period, the $\delta^{18}O$ record attains more constant values between the 7331–4002 cal. yr BP interval. The last period (4002–536 cal. yr BP) starts with a new abrupt change in the $\delta^{18}O$ values (from 1.90‰ to 1.75‰). After this decrease, the $\delta^{18}O$ record comes into a new relatively steady period with almost no significant variability until the upper part of the core. A general overview of the $\delta^{18}O$ record indicates the existence of at least two different stages or "modes of variability" in the area. Both modes illustrate different isotopic signatures, the former with relatively higher $\delta^{18}O$ values and the latter with relatively lower $\delta^{18}O$ values. The boundary between both modes is located at around 4000 cal. yr BP. This can also be recognized in the $\delta^{13}C$ record as a drastic event centered at ca. 4000 years and the change in the step-like decreasing $\delta^{13}C$ trend which is interrupted by a large sudden rises on $\delta^{13}C$ values (Figs. 2 and 3c).

4.2 Spectral analysis

Although spectral analyses were performed for both $\delta^{18}O$ and $\delta^{13}C$ records, significant results were only obtained in the case of the $\delta^{13}C$ record. This is probably caused by the low variability in the values of the $\delta^{18}O$. The CWS results of the $\delta^{13}C$ record in core EUGC-3B shows spectral variance maximum centred at ca. 1500 yr (Fig. 4b). Nevertheless, the spectral variance intensity decrease as we approach the margins of the spectrum, probably due to edge effects in the dataset and also to a lower time resolution in the early Holocene period. When compared to the other two selected proxy records, the pattern formerly depicted is repeated again. The HSG record from Core VM 29-191 shows significant spectral variance close to the 1500 yr periodicity (Fig. 4a), a fact previously described for this record (Bond et al., 1997, 1999). Finally, the CWS analysis of Hole 658C SST anomaly does not produce any strongly significant periodicity in the 1500 yr range, but a rather weaker spectral variance in this band (Fig. 4c).

5 Discussion

5.1 Hydrographic evolution in the Ría de Muros during the Holocene

Downcore variations of benthic foraminiferal stable isotopes in the Ría de Muros suggest that this area has experienced a set of major hydrographic changes during the last 8200 years. There are at least two different components forcing the variability in the EUGC-3B δ^{13}C record that need to be clearly identified. The overall trend present in the δ^{13}C record is interpreted to be caused by local changes in sea level, which induce changes in the supply of organic carbon to the seafloor as well as changes in water column ventilation rates. The general decrease of benthic δ^{13}C values from ca. 8200 to 4000 cal. yr BP is caused by the general sea level rise that took place in the Iberian Atlantic Margin from the Last Glacial Maximum (LGM) to the Holocene Climatic Optimum (HCO) ca. 5000 cal. yr BP (Dias et al., 2000), when sea level was a few meters above present. The sea level was located about 20 m below present sea level at about 8200 yr BP (Dias et al., 2000). As the water fills the basin of the ría, the primary production of the surface waters progressively increases as does the organic carbon flux to the sea floor so explaining the continuous decrease of benthic δ^{13}C values. From 4000 cal. yr BP onwards, overall δ^{13}C values continue relatively constantly as sea level approaches present values after the HCO (Dias et al., 2000).

The overall trend in the δ^{13}C record is punctuated by at least six (including the LIA) rapid millennial-scaled events of high δ^{13}C values (grey bars in Fig. 3). These δ^{13}C enrichments are probably linked with increased influence of the relatively more oxygenated ENACW$_{sp}$ over the Ría de Muros during enhanced upwelling periods. Upwelling of this water mass caused both more ventilation at the sea floor and an increase in the outwelling (export to the shelf) of the organic matter produced at this site. According to this model, more positive $\delta^{13}C$ values indicate more ventilation and less in-situ organic matter remineralization coinciding with periods of $ENACW_{sp}$ advection. Conversely, more negative $\delta^{13}C$ values account for reduced ventilation rates and enhanced in-situ organic matter degradation (i.e. decrease of the outwelling). These periods are related with the advection of the poorly oxygenated $ENACW_{st}$ (compared with the subtropical component) into the Ría de Muros (Fig. 3).

Although the centennial and millennial variability of the benthic $\delta^{18}O$ record has been to some extent reduced due to the opposite roles that salinity and temperature play in oxygen isotopes, the large scale changes in $\delta^{18}O$ record are the result of alterations in the relative influence of the two water masses bathing the Ría de Muros. The major shift in $\delta^{18}O$ towards heavier values at ca. 8200 cal. yr BP is interpreted to be the result of the establishment of full marine conditions in the Ría de Muros due to rapid sea level rise. After that initial period, the $\delta^{18}O$ record shows an abrupt change at ca. 4000 cal. yr BP that separates an early period with high $\delta^{18}O$ values from a late period with low $\delta^{18}O$ values indicating a change in the water mass that predominantly upwells into the Ría de Muros. According to this interpretation, the predominant water mass upwelling in the Ría de Muros during the early Holocene was the $ENACW_{st}$ whereas during the late Holocene the $ENACW_{sp}$ entered more frequently into the Ría de Muros. This shift from relatively warm and saltier to relatively cold and fresher waters is certainly in accordance with a general cooling trend throughout the Holocene as reported in many different paleo-records in this area (Marchal et al., 2002).

5.2 Links between high and low latitudes climatic patterns

Periods characterized by the presence of $ENACW_{sp}$ and strong upwelling events in the Ría de Muros (more positive benthic $\delta^{13}C$ values) correlate (within age model uncertainties) with cold SST anomalies off Cap Blanc (deMenocal et al., 2000b) (Fig. 3d). Such anomalies have been interpreted to be caused either by a southward advection of colder subpolar waters and/or by an intensification of large upwelling events that

CPD
3, 1283–1309, 2007

typically occur in this area (deMenocal et al., 2000b). Moreover, it has been previously proposed that these cooling events in the subtropical North Atlantic are directly linked with the HSG percentage fluctuations in the subpolar North Atlantic (Bond et al., 1997; deMenocal et al., 2000b). This strongly indicates that the presence of colder water masses and enhanced upwelling events entering into the Ría de Muros (i.e. increased influence of $ENACW_{sp}$) are strongly linked with North Atlantic cooling events associated with ice rafted debris episodes. Not surprisingly, both locations are directly under the influence of the western North Atlantic Subpolar-Subtropical Gyre (Canary Current). Therefore, any alteration in this regional system (i.e. intensification of northerly winds and/or southward displacement of the hydrographical fronts) should be recorded simultaneously in both areas. In the same way as North Atlantic polar front migrated southwards to a more zonal position during the LGM (Keffer et al., 1988), it is likely that minor cooling events in the North Atlantic induced similar southward displacements of the subpolar-subtropical gyre and the hydrographical fronts. Indeed, increased influence of $ENACW_{sp}$ into the Ría de Muros entails a southward displacement of the $ENACW_{sp}$/$ENACW_{st}$ front.

We suggest that these Holocene cold spells are propagated southward from the North Atlantic region by means of minor shifts in the general atmospheric and oceanic circulation patterns. Despite of the fact of that inaccuracies in the radiocarbon age model of core EUGC-3B could not enable to assess the synchronicity of those events, it has been argued that for the full suite of Holocene cooling events there is no any systematic temporal offset between subpolar and subtropical Atlantic within the calibrated radiocarbon chronologies (deMenocal et al., 2000b). In fact, the timing of the positive $\delta^{13}C$ excursions in core EUGC-3B shows a significant correlation (r^2=0.812) with the timing of the subtropical Atlantic SST anomalies record (Figs. 3a–d). Therefore, we conclude that the propagation of such cold episodes in the North Atlantic towards southern latitudes could have been nearly instantaneous, at least in terms of centennial-millennial scale changes. These relatively brief perturbations of the climatic system involved large-scale ocean and atmosphere reorganizations that were accomplished within centuries or perhaps decades.

5.3 Persistence of centennial-millennial scale climatic variability

Current radiocarbon chronologies in the selected records do not allow for assessing temporal leads-lags or time offsets in the three selected Atlantic areas. However, it might be possible to determine the persistence of these cycles and whether the paleo-records have been mainly dominated by global climatic cycles or by local and/or more regional influences.

Continuous wavelet time-frequency spectrums (Figs. 4a–c) illustrate that there is a general rhythmic pattern in the three time series with a mean periodicity of about 1500 yr, although the relative significance of the spectral signatures vary between the time series. Subpolar and mid-latitude records have been influenced by pervasive climate variability during the Holocene with a periodicity around 1500 yr as previously stated by several authors (O'Brien et al., 1995; Bond et al., 1997, 1999; Bianchi and McCave, 1999). The subtropical SST anomalies record spectral periods in the range of 1500 yr although the significances of these periods are quite low (Fig. 4c). Provided that the temporal resolution of this record should be enough to resolve centennial and millennial scale variability, it is likely that the influence of the northern 1500 yr cycle reaches these low latitudes somehow muted. Another possibility is that subtropical SST anomalies are affected by more regional hydrographic changes. In fact, Hole 658C is under the influence of the African monsoon, which in turn is controlled by insolation changes (deMenocal et al., 2000a; Kuhlmann et al., 2004). Hence, during time periods of strong subtropical monsoon the subpolar signal might be to some extent veiled, or perhaps completely erased from the sediment record. It has been widely recognized that the Holocene records of low latitudes has been strongly forced by monsoon processes (Neff et al., 2001; Fleitmann et al., 2003; Russell and Johnson, 2005). These factors could explain the lower contribution of these rhythmic climatic changes during the Holocene. On the contrary, the EUGC-3B δ^{13}C record (located at a mid point between the subtropical SST record and the subpolar HSG %) is strongly affected by the

CPD

3, 1283–1309, 2007

1500 yr cycles (Fig. 4b). It seems, therefore, that the primary origin of the 1500 yr periodicity is placed somewhere at the Northern Hemisphere high latitudes and that signal is rapidly (sub-centennially) propagated southward where its effects are weakened or perhaps dampened by low latitude climatic processes (e.g. African monsoon). Further support for these interpretation comes from a recent work in the Alboran Sea (Western Mediterranean Sea) which clearly establish a dissimilarity in spectral patterns between marine-based proxies (biomarkers SSTs presenting a significant 1500 yr periodicity) and land-based proxies (i.e. Saharian dust input without significant 1500 yr periodicity)(Moreno et al., 2005).

6 Conclusions

The analyses of benthic foraminiferal stable isotopes in gravity core EUGC-3B has allowed the reconstruction of the Holocene paleoceanographic history of the NW Iberian Margin.

Benthic foraminiferal oxygen and carbon isotopes register the predominant water mass advection and/or upwelling into the Ría de Muros for the last 8200 cal. yr. BP. Oxygen isotopes indicate that the Early Holocene (8200–4000 cal. yr. B.P) was mainly influenced by $ENACW_{st}$ whereas the late Holocene (4000–500 cal. yr. B.P) was affected by $ENACW_{sp}$. More negative $\delta^{13}C$ values correspond to the presence of $ENACW_{st}$, reduced ventilation rates and increased in-situ organic matter degradation. Six major benthic foramniferal positive $\delta^{13}C$ isotopic events were registered for the last 8200 cal. yr BP, clearly indicating the presence of cold and well ventilated $ENACW_{sp}$ and increased exportation of organic carbon to the adjacent continental shelf. We have interpreted these isotopic excursions as northward and southward migrations of the hydrographical front between both water masses in the area, the Finisterre Front.

There is a clear link between these cold events in the Ría de Muros and more widespread Holocene centennial-millennial time scale climatic perturbations at high and low latitudes in the North Atlantic region. Spectral analyses indicate that these events present a recurrent 1500 yr periodicity throughout the Holocene. These cold episodes are likely triggered at high latitudes and then rapidly propagated towards lower latitudes by means of southwards shifts of atmospheric and oceanic circulatory systems. This periodicity is somewhat diluted as it approaches lower latitudes, being superimposed by regional climatic and oceanographic features as well as by more general low latitude processes.

Acknowledgements. The authors acknowledge to the EU project HOLSMEER: Holocene Shallow Marine Environments of Europe (EVK2-CT-2000-00060) for providing samples and financial support. L. Pena and P. Diz also thank the Paleostudies Program (Geosciences Faculty, Bremen University, Germany) for providing us with analytical facilities, and to F. Lamy for all the help provided. We wish to thank also M. Segl for the help with the IRMS measurements. L. Pena acknowledges a fellowship from the Comer Abrupt Climate Change Foundation (USA). Thoughtful comments and discussion provided by I. Cacho and P. G. Mortyn are greatly thanked.

References

Álvarez-Salgado, X. A., Castro, C. G., Pérez, F. F., and Fraga, F.: Nutrient mineralization patterns in shelf waters of the western Iberian upwelling, Cont. Shelf Res., 17, 1247–1270, 1997.

Álvarez-Salgado, X. A., Figueiras, F. G., Pérez, F. F., Groom, S., Nogueira, E., Borges, A. V., Chou, L., Castro, C. G., Moncoiffé, G., Ríos, A. F., Miller, A. E. J., Frankignoulle, M., Savidge, G., and Wollast, R.: The Portugal coastal counter current off NW Spain: new insights on its biogeochemical variability, Prog. Oceanogr., 56, 281–321, 2003.

Álvarez-Salgado, X. A., Gago, J., Míguez, B. M., Gilcoto, M., and Pérez, F. F.: Surface watern of the NW Iberian margin: Upwelling on the shelf versus Outwelling of upwelled waters from the Rías Baixas, Estuarine, Coastal and Shelf Science, 51, 821–837, 2000.

Álvarez-Salgado, X. A., Rosón, G., Pérez, F. F., and Pazos, Y.: Hydrographic variability off the Rías Baixas (NW Spain) during the upwelling season, J. Geophys. Res., 98, 14 447–14 455, 1993.

Álvarez, M., Flores, J. A., Sierro, F. J., Diz, P., Francés, G., Pelejero, C., and Grimalt, J. O.:

Millennial surface water dynamics in the Ría de Vigo during the last 3000 years as revealed by coccoliths and molecular biomarkers, Palaeogeogr. Palaeocl., 218, 1–13, 2005.
Andrews, J. T., Hardadottir, J., Stoner, J. S., Mann, M. E., Kristjansdottir, G. B., and Koc, N.: Decadal to millennial-scale periodicities in North Iceland shelf sediments over the last 12 000 cal yr: long-term North Atlantic oceanographic variability and solar forcing, Earth Planet. Sc. Lett., 210, 453–465, 2003.
Bianchi, G. G. and McCave, I. N.: Holocene periodicity in North Atlantic climate and deep-ocean flow south of Iceland, Nature, 397, 515–517, 1999.
Bond, G., Kromer, B., Beer, J., Muscheler, R., Evans, M. N., Showers, W., Hoffmann, S., Lotti-Bond, R., Hajdas, I., and Bonani, G.: Persistent Solar Influence on North Atlantic Climate During the Holocene, Science, 294, 2130–2136, 2001.
Bond, G., Showers, W., Cheseby, M., Lotti, R., Almasi, P., deMenocal, P., Priore, P., Cullen, H., Hajdas, I., and Bonani, G.: A pervasive millenial-scale cycle in North Atlantic Holocene and glacial climates, Science, 278, 1257–1266, 1997.
Bond, G., Showers, W., Elliot, M., Evans, M. N., Lotti, R., Hajdas, I., Bonani, G., and Johnson, S.: The North Atlantic's 1–2 kyr climate rhythm: Relation to Heinrich Events, Dansgaard/Oeschger and the Little Ice Age, in: Mechanisms of global climate change at millennial time scales, edited by: Clark, P.U., Webb, R. S., and Keigwin, L. D., pp. 35–58, Geophysical Monograph, American Geophysical Union, Washington, 1999.
Braun, H., Christl, M., Rahmstorf, S., Ganopolski, A., Mangini, A., Kubatzki, C., Roth, K., and Kromer, B.: Posible solar origin of the 1 470-year glacial climate cycle demonstrated in a coupled model, Nature, 438, 208–211, 2005.
Campbell, I. D., Campbell, C., Apps, M. J., Rutter, N., and Bush, A. B. G.: Late Holocene ~1500 yr climatic periodicities and their implications, Geology, 26, 471–473, 1998.
Castro, C. G., Pérez, F. F., Álvarez-Salgado, X. A., Rosón, G., and Ríos, A. F.: Hydrographic conditions associated with the relaxation of an upwelling event off the Galician coast (NW Spain), J. Geophys. Res., 99, 5135–5147, 1994.
Conkright, M. E., Locarnini, R. A., Garcia, H. E., O'Brien, T. D., Boyer, T. P., Stephens, C., and Antonov, J. I.: World Ocean Atlas 2001: Objective Analyses, Data Statistics, and Figures, CD-ROM Documentation, Silver Spring, 2002.
deMenocal, P., Ortiz, J., Guilderson, T. P., Adkins, J., Sarnthein, M., Baker, L., and Yarusinsky, M.: Abrupt onset and termination of the African Humid Period: rapid climate responses to gradual insolation forcing, Quaternary Sci. Rev., 19, 347–361, 2000a.

deMenocal, P., Ortiz, J., Guilderson, T. P., and Sarnthein, M.: Coherent high- and low-climate variability during the Holocene warm period, Science, 288, 2198–2202, 2000b.
Desprat, S., Sánchez-Goñi, M. F., and Loutre, M. F. Revealing climatic variability of the last three millennia in northwestern Iberia using pollen influx data, Earth Planet. Sc. Lett., 213, 63–78, 2003.
Dias, J. M. A., Boski, R., Rodrigues, A., and Magalhaes, F.: Coast line evolution in Portugal since the Last Glacial Maximum until present–a synthesis, Mar. Geol., 170, 177–186, 2000.
Diz, P., Francés, G., Pelejero, C., Grimalt, J. O., and Vilas, F.: The last 3000 years in the Ría de Vigo (NW Iberian Margin): climatic and hydrographic signals, The Holocene, 12, 383–392, 2002.
Diz, P. and Francés, G.: Distribution of live benthic foraminifera in the Ría de Vigo, Mar. Micropaleontol., in press, 2007.
Fiúza, A. F. G.: Hidrologia e dinâmica das aguas costeiras de Portugal, PhD. Thesis, Universidade de Lisboa, 1984.
Fiúza, A. F. G., Hamann, M., Ambar, I., Díaz del Río, G., González, N., and Cabanas, J. M.: Water masses and their circulation off western Iberia during May 1993, Deep-Sea Res. I, 45, 1127–1160, 1998.
Fleitmann, D., Burns, S. J., Mudelsee, M., Neff, U., Kramers, J., Mangini, A., and Matter, A.: Holocene Forcing of the Indian Monsoon Recorded in a Stalagmite from Southern Oman, Science, 300, 1737–1739, 2003.
Fraga, F.: El afloramiento costero en la costa atlántica de la Península Ibérica., Revista Academia Galega de Ciencias, X, 144–152, 1991.
Ghil, M., Allen, M. R., Dettinger, M. D., Ide, K., Kondrashov, D., Mann, M. E., Robertson, A. W., Saunders, A., Tian, Y., Varadi, F., and Yiou, P.: Advanced spectral methods for climatic time series, Rev. Geophys., 40, 1–41, 2002.
Giraudeau, J., Cremer, M., Manthé, S., Labeyrie, L. D., and Bond, G. Coccolith evidence for instabilities in surface circulation south of Iceland during Holocene times, Earth Planet. Sc. Lett., 179, 257–268, 2001.
González-Álvarez, R., Bernárdez, P., Pena, L. D., Francés, G., Prego, R., Diz, P., and Vilas, F. Paleoclimatic evolution of the Galician continental shelf (NW of Spain) during the last 3000 years: from a storm regime to present conditions, J. Marine Syst., 54, 245–260, 2005.
Hall, I., Bianchi, G. G., and Evans, J. R.: Centennial to millennial scale Holocene climate-deep water linkage in the North Atlantic, Quaternary Sci. Rev., 23, 1529–1536, 2004.

Hu, F. S., Kaufman, D., Yoneji, S., Nelson, D., Shemesh, A., Huang, Y., Tian, J., Bond, G., Clegg, B., and Brown, T.: Cyclic Variation and Solar Forcing of Holocene Climate in the Alaskan Subartic, Science, 301, 1890–1893, 2003.

Keffer, T., Martinson, D. G., and Corliss, B. H.: The position of the Gulf Stream during Quaternary glaciations, Science, 241, 440-442, 1988.

Keigwin, L. D., and Boyle, E. A.: Detecting Holocene changes in thermohaline circulation, PNAS, 97, 1343–1346, 2000.

Kuhlmann, H., Meggers, H., Freudenthal, T., and Wefer, G.: The transition of the monsoonal and the N Atlantic climate system off NW Africa during the Holocene, Geophys. Res. Lett., 31, 2004.

Lebreiro, S. M., Francés, G., Abrantes, F. F. G., Diz, P., Bartels-Jonsdottir, H.B., Stroynowski, Z., Gil, I. M., Pena, L. D., Rodrigues, T., Nombela, M. A., Alejo, I., Briffa, K., Jones, P., and Harris, I.: Last two millennia coastal hydrographic and climate changes in the Atlantic Iberian margin (Tagus prodelta and Ría de Muros), The Holocene, 16, 1003–1015, 2006.

Lomb, N. R.: Least-squares frequency analysis of unequally spaced data, Astrophys. Space Sci., 39, 447–462, 1976.

Mann, M. E. and Lees, J. M.: Robust estimation of background noise and signal detection in climatic time series, Climatic Change, 33, 409–445, 1996.

Marchal, O., Cacho, I., Stocker, T. F., Grimalt, J. O., Calvo, E., Martrat, B., Shackleton, N.J., Vautravers, M., Cortijo, E., van Kreveld, S. A., Andersson, C., Koç, N., Chapman, M. R., Sbaffi, L., Duplessy, J. C., Sarnthein, M., Turon, J. L., Duprat, J. and Jansen, E.: Apparent long-term cooling of the sea surface in the Northeast Atlantic and Mediterranean during the Holocene, Quaternary Sci. Rev., 21, 455–483, 2002.

Marchitto, T. M. and deMenocal, P.: Late Holocene variability of upper North Atlantic Deep Water temperature and salinity, Geochem. Geophy. Geosy., 4, 2003.

Martínez-Cortizas, A., Pontevedra-Pombal, X., García-Rodeja, E., Nóvoa-Muñoz, J. C., and Shotyk, W.: Mercury in a Spanish Peat Bog: Archive of Climate Change and Atmospheric Metal Deposition, Science, 284, 939–942, 1999.

McCartney, M. S. and Talley, L. D.: The Subpolar Mode Water of the North Atlantic Ocean, J. Phys. Oceanogr., 12, 1169–1188, 1982.

McDermott, F., Mattey, D. P., and Hawkesworth, C. J.: Centennial-scale Holocene climate variability revealed by a High-Resolution speleotherm $\delta^{18}O$ record from SW Ireland, Science, 294, 1328–1331, 2001.

Moreno, A., Cacho, I., Canals, M., Grimalt, J. O., Sánchez-Goñi, M. F., Shackleton, N., and Sierro, F. J.: Links between marine and atmospheric processes oscillating on a millennial time-scale. A multi-proxy study of the last 50 000 yr from the Alboran Sea (Western Mediterranean Sea), Quaternary Sci. Rev., 24, 1623–1636, 2005.

Murray, J. W.: Ecology and Paleoecology of Benthic Foraminifera, Longman, Avon, 1991.

Neff, U., Burns, S. J., Mangini, A., Mudelsee, M., Fleitmann, D., and Matter, A.: Strong coherence between solar varability and the monsoon in Oman between 9 and 6 kyr, Nature, 411, 290–293, 2001.

O'Brien, S. R., Mayewski, P. A., Meeker, L. D., Meese, D. A., Twickler, M. S., and Whitlow, S. I.: Complexity of Holocene Climate as Reconstructed from a Greenland Ice Core, Science, 270, 1962–1964, 1995.

Oppo, D. W., McManus, J. F., and Cullen, J. L.: Deepwater variability in the Holocene epoch, Nature, 422, 277–278, 2003.

Peliz, A., Rosa, T. L., Santos, A. M., and Pissarra, J. L.: Fronts, jets, and counter-flows in the Western Iberian upwelling system, J. Mar. Systems, 35, 61–77, 2002.

Percival, D. B. and Walden, A. T.: Spectral Analysis for Physical Applications, Cambridge Universtiy Press, Cambridge UK, 1993.

Pérez, F. F., Castron, C. G., Álvarez-Salgado, X. A., and Ríos, A. F.: Coupling between the Iberian basin–scale circulation and the Portugal boundary current system: a chemical study, Deep-Sea Research I, 48, 1519–1533, 2001.

Pérez, F. F., Mouriño, C., Fraga, F., and Ríos, A. F.: Displacement of water masses and remineralization rates off the Iberian Peninsula by nutrient anomalies, J. Mar. Res., 51, 869–892, 1993.

Ríos, A. F., Pérez, F. F., and Fraga, F.: Water masses in the upper and middle North Atlantic Ocean east of the Azores, Deep-Sea Res., 39, 645–658, 1992.

Russell, J. M. and Johnson, T. C.: A high-resolution geochemical record from Lake Edward, Uganda Congo and the timing and causes of tropical African drought during the late Holocene, Quaternary Sci. Rev., 24, 1375–1389, 2005.

Schulz, M. and Paul, A.: Holocene Climate Variability on Centennial-to-Millennial Time Scales: 1. Climate Records from the North-Atlantic Realm, in: Climate Development and History of the North Atlantic Realm, edited by: Wefer, G., Berger, W. H., Behre, K.-E., and Jansen, E., pp. 41–54, Springer-Verlag, Berlin, 2002.

Soares, A. M.: Variabilidade do "upwelling" costeiro durante o Holocénico nas margens

Atlânticas ocidental e meridional da Península Ibérica, PhD Thesis, University of Algarve (Portugal), 205 pp., 2004.
Solignac, S., de Vernal, A., and Hillaire-Marcel, C.: Holocene sea-surface conditions in the North Atlantic-contrasted trends and regimes in the western and eastern sectors (Labrador Sea vs. Iceland Basin), Quaternary Sci. Rev. , 23, 319–334, 2004.
Stuiver, M. and Reimer, P. J.: Extended ^{14}C data base and revised CALIB 3.0^{14}C age calibration program, Radiocarbon, 35, 215–230, 1993.
Thomson, D. J.: Spectrum estimation and harmonic analysis, Proceedings of IEEE, 70, 1055–1096, 1982.
Torrence, C. and Compo, G. P.: A Practical Guide to Wavelet Analysis, B. Am. Meteorol. Soc., 79, 61–78, 1998.
Varela, R. A., Rosón, G., Herrera, J. L., Torres-López, S., and Fernández-Romero, A.: A general view of the hydrographic and dynamical patterns of the Rías Baixas adjacent sea area, J. Mar. Systems, 54, 97–113, 2005.
Viau, A. E., Gajewski, K., Fines, P., Atkinson, D. E., and Sawada, M. C.: Widespread evidence of 1500 yr climate variability in North America during the past 14 000 yr, Geology, 30, 455–458, 2002.

CPD

3, 1283–1309, 2007

EGU

Table 1. AMS radiocarbon dated levels from core EUGC-3B. All the analyses were performed at the AMS Laboratory, Institute of Physics and Astronomy (University of Aarhus, Denmark). Raw radiocarbon 14C ages were $\delta^{13}C$ corrected and calibrated to calendar ages using the Calib 5.01 program (Stuiver and Reimer, 1993).

Sample (cm)	Sample type	^{14}C Age (BP)	Calibrated age± 2 stdv.	$\delta^{13}C$ (‰) VPDB
EUGC-3B (1)	Benth. Foram. (Nonion commune)	920±65	[435–638 cal. BP] (536 cal. BP)	−2.53
EUGC-3B (57)	Bivalve Shell (Venus nux)	1229±39	[682–879 cal. BP] (780 cal. BP)	−1.97
EUGC-3B (93)	Bivalve Shell (Myrtea spinifera)	1575±40	[1035–1246 cal. BP] (1140 cal. BP)	−0.84
EUGC-3B (178)	Bivalve Shell (Myrtea spinifera)	2623±45	[2154–2430 cal. BP] (2292 cal. BP)	−0.14
EUGC-3B (238)	Bivalve Shell (Venus nux)	3355±55	[3057–3357 cal. BP] (3207 cal. BP)	−0.04
EUGC-3B (321)	Bivalve Shell (Myrtea spinifera)	4805±50	[4922–5266 cal. BP] (5094 cal. BP)	0.17
EUGC-3B (407)	Bivalve Shell (Lucinoma borealis)	7610±60	[7938–8194 cal. BP] (8066 cal. BP)	2.23

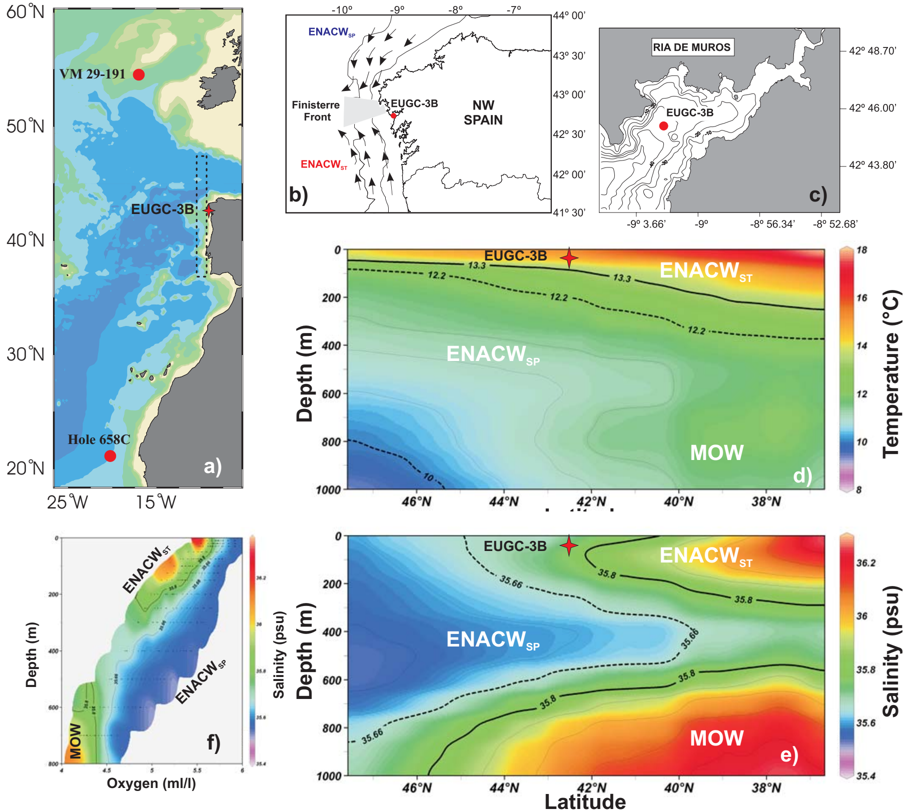
60°N
50°N
40°N
30°N
20°N
25°W
15°W
VM 29-191
EUGC-3B
Hole 658C
a)
-10°
-9°
-8°
-7°
44° 00'
43° 30'
43° 00'
42° 30'
42° 00'
41° 30'
ENACW$_{SP}$
Finisterre Front
EUGC-3B
NW SPAIN
ENACW$_{ST}$
b)
RIA DE MUROS
EUGC-3B
42° 48.70'
42° 46.00'
42° 43.80'
-9° 3.66'
-9°
-8° 56.34'
-8° 52.68'
c)
EUGC-3B
ENACW$_{ST}$
ENACW$_{SP}$
MOW
Depth (m)
Temperature (°C)
46°N
44°N
42°N
40°N
38°N
d)
ENACW$_{ST}$
ENACW$_{SP}$
MOW
Depth (m)
Salinity (psu)
Oxygen (ml/l)
f)
EUGC-3B
ENACW$_{ST}$
ENACW$_{SP}$
MOW
Depth (m)
Salinity (psu)
Latitude
e)

Fig. 1.

Fig. 1. **(a)** Map showing the location of core site EUGC-3B (42° 45′N, 09° 02′W, 38 m water depth) and the two other North Atlantic core sites selected for comparison, VM 29-191 (54° 16′N, 16° 47’W, 2370 m water depth, Bond et al., 1997) and ODP Site 658C (20° 45′N, 18° 35′W, 2263 m water depth, Cape Blanc, Mauritania, deMenocal et al., 2000b). **(b)** Schematic representation of the subsurface hydrographic front formed between $ENACW_{sp}$ and $ENACW_{st}$ (Fraga, 1991) over the continental shelf in the vicinity of Cape Finisterre and close to the location of core EUGC-3B. **(c)** Detailed bathymetric chart of the Ría de Muros (NW Spain) and core site EUGC-3B. **(d–e)** Hydrographic section of the western Iberian Margin illustrating the mean annual temperature and salinity fields that characterize $ENACW_{sp}$ and $ENACW_{st}$ water masses (Conkright et al., 2002). Isotherms and isohalines plotted as defined by Fiúza (1984). MOW: Mediterranean Outflow Water. The red star shows the location of core EUGC-3B between the two water masses. **(f)**Triple plot of depth (m), oxygen concentration (ml/l) and salinity (psu) from western Iberia Margin. Note that for a constant depth, $ENACW_{sp}$ is relatively more oxygenated than $ENACW_{st}$ (Conkright et al., 2002).

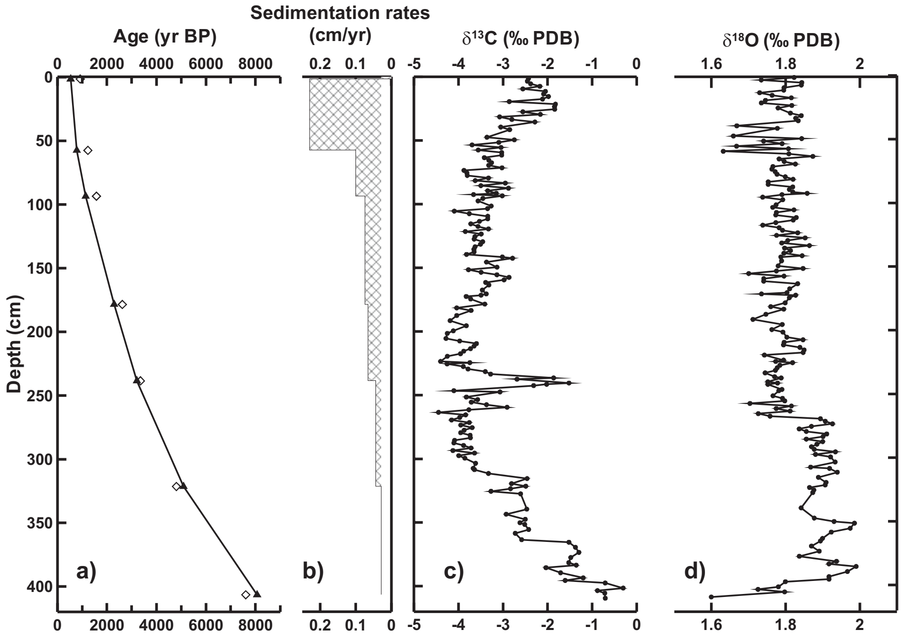

Fig. 2. Compilation of data from core EUGC-3B. **(a)** Age model based on 7 AMS radiocarbon dates (see Table 1 for details). Open diamonds are raw radiocarbon ages whereas black triangles are marine reservoir calibrated ages. All ages are expressed in cal. yr BP. **(b)** Sedimentation rates (cm/yr). **(c)** Benthic foraminifera (Nonion commune) δ^{13}C record vs. depth. **(d)** Benthic foraminifera (Nonion commune) δ^{18}O record vs. depth.

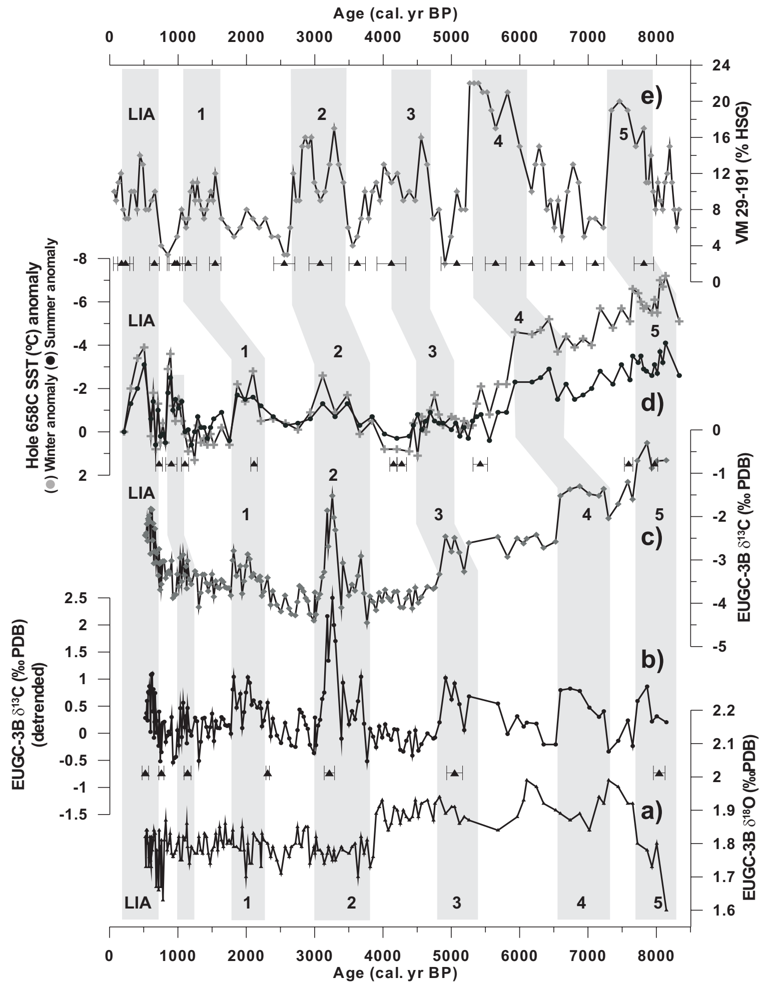

Fig. 3. Continued.

CPD
3, 1283–1309, 2007

Holocene climate variability in NW Iberia

L. D. Pena et al.

EGU

Fig. 3. Comparison of the **EUGC-3B** benthic foraminiferal $\delta^{18}O$ and $\delta^{13}C$ records **(a–c)** with two other North Atlantic records: **(d)** Sea Surface Temperature anomalies for the warm and cold seasons from ODP Site 658C (20° 45′N, 18° 35′W, 2263 m water depth, Cape Blanc, Mauritania, deMenocal et al., 2000b) and **(e)** Hematite Stained Grains percentage (%HSG) of core VM 29-191 (54° 16′N, 16° 47′W, 2370 m water depth, Bond et al., 1997). Radiocarbon ages (cal. yr BP) and uncertainty bars are shown for each record. Grey bands illustrate the correlation between cold periods in these three records, with periods of predominant $ENACW_{sp}$ at the NW Iberian Margin linked to colder SST anomalies in the subtropical North Atlantic and higher percentages of HSG in the subpolar North Atlantic. Bold numbers refer to the Holocene cold events (Bond et al., 1997). LIA: Little Ice Age.

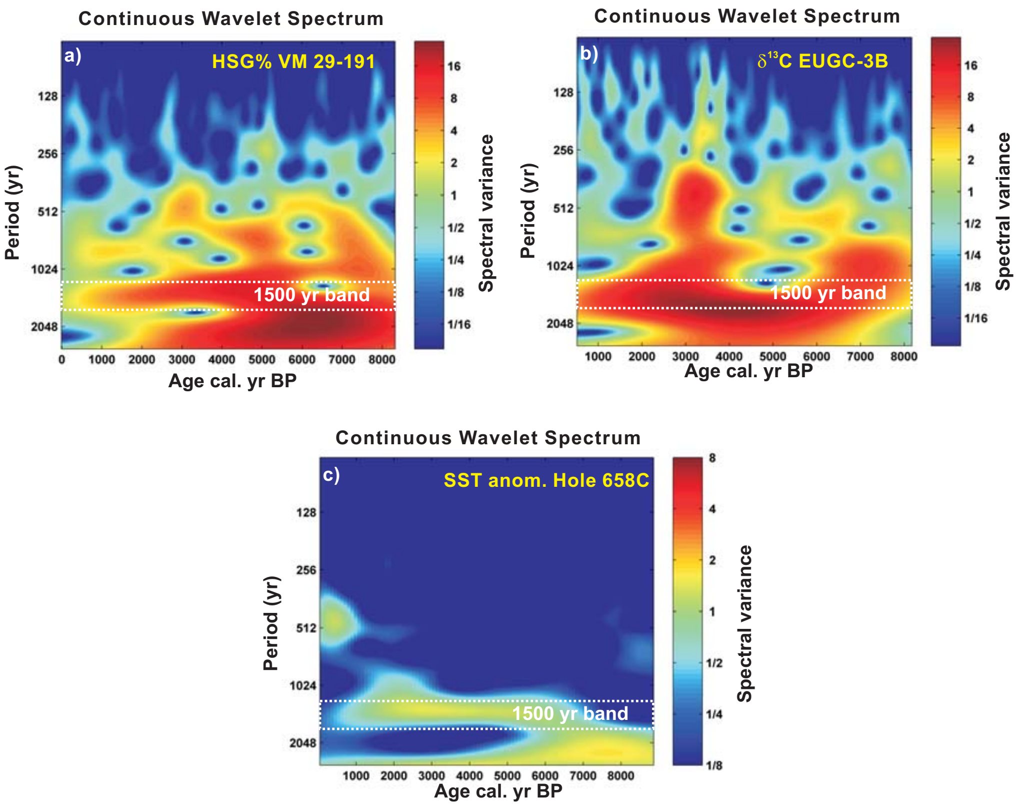

Fig. 4. Multiple spectral analyses of the selected records. As a routine, linear trends were removed in every data-set before running spectral analysis in order to reduce red noise (i.e. background power decreases with increasing frequencies). **(a–c)** Continuous Wavelet Spectrum (CWS) illustrating the spectral variance through time in the three selected records. Colour scales show the different spectral variances intensities for each plot. Vertical axes represent periods (yr) computed at every single time step of the time series.